Atom Indonesia

Journal homepage: http://atomindonesia.brin.go.id

Image Quality Assessment of Hybrid Statistical Iterative Reconstruction (H/SIR) in Comparison to Filtered Back Projection (FBP)

H. Arjah[1,2], N. D. Osman[1*], H. ALMasri[3], C. Anam[4], M. E. Aziz[5]

[1]*Advanced Medical and Dental Institute, Universiti Sains Malaysia, Kepala Batas, Penang, Malaysia*
[2]*Radiology Departement, Allmed Medical Center Ramallah, Palestine*
[3]*Medical Imaging Departement, Al-Quds University, Abu dis, Jerusalem, Palestine*
[4]*Department of Physics, Faculty of Sciences and Mathematics, Diponegoro University, Jl. Prof. Soedarto SH Tembalang, Semarang 50275, Central Java, Indonesia*
[5]*Department of Radiology, School of Medical Sciences, Universiti Sains Malaysia, Kubang Kerian, Kelantan Malaysia*

ARTICLE INFO

Article history:
Received 12 September 2024
Received in revised form 17 February 2025
Accepted 24 February 2025

Keywords:

Computed tomography
Low dose
Iterative reconstruction

ABSTRACT

Hybrid Statistical Iterative Reconstruction (H/SIR) is a method for Computed Tomography (CT) image reconstruction that provides optimal diagnostic images while reducing radiation doses compared to the standard protocol using Filtered Back Projection (FBP). This work aims to assess the image quality metrics; Signal to Noise Ratio (SNR) and Contrast-to-Noise Ratio (CNR) of Low-Dose Computed Tomography (LDCT) examination with different vendors H/SIR algorithms. Three CT scanners from different manufacturers (Philips, GE, and Siemens) were used in this work. A total of 218 clinical images were analysed. The SNR and CNR of LDCT+H/SIR images were compared with standard protocol combined with FBP. The quantitative assessments were achieved by IndoQCT software. Results showed that H/SIR preserved image quality while radiation dose was minimized.

© 2026 Atom Indonesia. All rights reserved

INTRODUCTION

The rapid advancement of multidetector CT imaging has made CT scans a preferred diagnostic tool, increasing their use significantly over the past decade. However, this has raised concerns about the risks of ionizing radiation, such as cancer from high radiation doses. CT scans account for about 66% of all medical radiation exposure, and the cumulative radiation from CT can raise the risk of cancer.

Several approaches adopted to reduce radiation dose, such as automatic tube current modulation, automatic kilovoltage (kVp) or mAs selection, and dynamic z-axis beam collimation, have been used to reduce CT-associated radiation dose. However, these methods have limited effectiveness when the Filtered Back Projection (FBP) algorithm is used for image reconstruction. FBP algorithm results in streak artifacts and increased noise in low-dose images [1,2]. Modified CT protocols are employed by editing the scanning parameters and lowering the tube mAs and kVp [3]. However, the main drawback of lowering the radiation dose is the increased image noise, which can affect the diagnostic quality of the image [4].

Another approach for optimizing radiation dose is the use of the Iterative Reconstruction (IR) algorithm. The IR algorithm is one of the most important advancements in CT for improving image quality by eliminating artefacts and subtracting noise. CT system manufacturers have proposed different models of Iterative Reconstruction (IR) algorithms, such as Model-Based Iterative Reconstruction (MBIR) and Hybrid Statistical Iterative Reconstruction (H/SIR). The H/SIR algorithm, used in this work, combines both Filtered Back Projection (FBP) and Iterative Reconstruction at various levels [5]. The H/SIR algorithm adopted by the Philips CT scanner is iDose^4 [6], the GE CT scanner is Adaptive Statistical iterative Reconstruction-Voe (ASiR-V) [7], and the Siemens is Sinogram Affirmed Iterative Reconstruction

*Corresponding author.
E-mail address: noordiyana@usm.my
DOI: https://doi.org/10.55981/aij.2026.1528

(SAFIRE) [8]. These algorithms operate in both data space and image space. They first correct the sinograms and then reduce image noise through denoising or noise subtraction while preserving edges to maintain image resolution [6,7,9]. These algorithms effectively reduce noise associated with lower radiation doses and provide better image quality compared to FBP images obtained using standard protocols [1]. Siemens SOMATOM go.NOW CT scanners employ iterative Beam Hardening Correction (iBHC) to eliminate beam hardening artefacts in head CT [10].

Visualizing low-contrast lesions, such as those in early stroke, is one of the most challenging tasks in CT imaging. Therefore, it is essential to assess the Low-Contrast Detectability (LCD) performance of different IR algorithms under routine clinical CT settings before applying a dose reduction technique [2]. However, the Contrast-to-Noise Ratio (CNR) can be used as an index for assessing LCD [11].

The volume-weighted CT Dose Index ($CTDI_{vol}$) is the standard measure of radiation exposure in CT exams. For brain CT, a 16 cm head phantom is used to estimate $CTDI_{vol}$. However, $CTDI_{vol}$ can be inaccurate because actual patient sizes vary from the standard phantom. As the patient's size decreases, their radiation exposure increases [12]. If $CTDI_{vol}$ remains constant across different patient sizes, the Signal-to-Noise Ratio (SNR) and CNR will vary due to differences in absorbed doses [13].

Minimizing $CTDI_{vol}$ in brain LDCT is challenging because clear visualization of gray-white matter is essential for diagnosing subtle lesions or pathologies. Differentiating Gray Matter (GM) and White Matter (WM), which have only a 6–7 Hounsfield Unit (HU) attenuation difference, requires optimal low-contrast resolution. Reducing the radiation dose can worsen the GM-WM differentiation due to increased noise from fewer X-ray photons reaching the detector. The main issue is that as the image noise increases, low-contrast resolution significantly degrades, limiting the potential for dose reduction in brain CT [14].

This work aims to assess the image quality for the Low-Dose CT (LDCT) protocol in combination with the H/SIR algorithm compared to standard dose CT protocols. The SNR and CNR of GM and WM in clinical images are compared between the two protocols (LDCT-H/SIR and SDCT-FBP).

METHODS

A total of 218 clinical CT images of the brain CT scans were collected and analyzed. This study involves data from three CT scanners of different vendors, including Philips Ingenuity Core (Philips Healthcare, Cleveland, OH), Siemens SOMATOM go.NOW® (Siemens Healthcare, Forchheim, Germany), and GE Revolution™ (GE Healthcare, Milwaukee, WI). All clinical images were obtained and reconstructed using two different protocols in each scanner: the Standard Dose CT protocols combined with FBP (SDCT-FBP), and Low Dose CT protocols combined with H/SIR (LDCT-H/SIR). The exposure settings for both protocols and the number of patients (N) are summarized in Table 1. For Siemens datasets, the images were reconstructed with FBP and IR in combination with an iterative Beam Hardening Correction (iBHC) algorithm.

The image quality of the clinical CT images was quantitatively assessed using IndoQCT software (developed by Anam et al., 2017) [15]. Two Regions of Interest (ROIs) were placed on White Matter (WM) and Gray Matter (GM) to evaluate SNR and CNR of WM to GM (CNR_{WM-GM}), as shown in Fig. 1. The ROI was placed on the left thalamus deep GM and left frontal WM, then measurements were repeated on the right side, and the average of both ROI for WM or GM was obtained.

The SD of HU is used as a noise index and measured according to Eq. (1). The ROI size was fixed at 20 pixels.

$$SD = \sqrt{\frac{\sum_{i=1}^{n}(x_i-\mu)^2}{n-1}} \quad (1)$$

Table 1. Scanning parameters and the number of patients for each scanner.

CT scanners	N	Protocols	Mean $CTDI_{vol}$ (mGy)	Reconstruction algorithm
Philips	35	Low Dose	32.29	iDose4
	46	Standard Dose	61.09	FBP
Siemens	37	Low Dose	30.40	SAFIRE-iHBC
	37	Standard Dose	56.79	FBP-iHBC
GE	31	Low Dose	35.96	ASiR-V
	32	Standard Dose	82.35	FBP

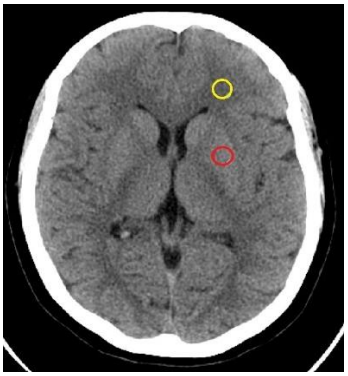

Fig. 1. Two ROIs marked at the thalamus deep GM. and frontal WM.

Where x_i is the pixel value or HU within the ROI, μ is the average pixel value or mean HU, and n is the number of pixels within the ROI. The SNR value of WM and GM was determined by dividing the mean HU that represents the Signal Intensities (SI) of ROI by the SD of HU, which represents the noise according to Eq. (2) [16].

$$SNR = \frac{HU_{mean}}{SD} \quad (2)$$

HU_{mean} is the mean HU for all pixels inside the ROI, and SD is the SD of HU within the ROI. The CNR of WM to GM is determined using Eq. (3).

$$CNR = \frac{HU_{GM} - HU_{WM}}{\sqrt{SD_{GM}{}^2 + SD_{WM}{}^2}} \quad (3)$$

The SNR per radiation dose (SNRD) and CNR per radiation dose (CNRD) were calculated using Eqs. (4) and (5). In this work, the SNRD and CNRD measure the SNR and CNR normalization radiation dose, $CTDI_{vol}$ [17].

$$SNRD = \frac{SNR}{\sqrt{CTDI_{vol}}} \quad (4)$$

$$CNRD = \frac{CNR}{\sqrt{CTDI_{vol}}} \quad (5)$$

Both metrics reflect how well contrast can be detected in the image relative to the dose used. These metrics are essential in dose optimization studies, where dose savings must be carefully balanced with diagnostic image quality. A higher SNRD or CNRD means better image quality for a given dose.

The statistical analysis was conducted using paired Student's t-tests to compare the quantitative image quality metrics, including SNR, CNR, SNRD, and CNRD between the between the evaluated CT protocols. If the p-value is less than 0.001 (the specified α level), it indicates a statistically significant difference in the mean image quality parameters.

RESULTS AND DISCUSSION

Signal-to-Noise Ratio (SNR)

Figure 2 shows boxplots for SNR distribution for WM (top) and GM (bottom) between different CT scanners and CT protocols (SDCT-FBP and LDCT-H/SIR). From the graph, it can be observed that for the Philips CT scanner, the LDCT combined with iDose^4 increased the SNR_{WM} with an average value of 11.8, compared to SDCT-FBP with an average SNR_{WM} of 10.5. However, the difference was not statistically significant ($p > 0.001$).

For Siemens and GE CT, both exhibited lower SNR_{WM} for LDCT as compared to SDCT. In Siemens scanner, the average SNR_{WM} was 11.33 for LDCT protocol combined with SAFIRE, as compared to SDCT-FBP, with an average of 12.69. In the GE scanner, the SNR_{WM} was 7.6 for LDCT combined with ASiR-V, which was significantly lower ($p < 0.001$) than SDCT-FBP with an average SNR of 9.5.

There was no significant difference in SNR_{WM} between the low dose and standard protocol of Philips and Siemens, while GE exhibited a significant increment of SNR_{WM} for LDCT, which used a tube voltage of 100 kVp.

A similar work was concluded by Sun et al., which employed ASiR-V on brain CT and reported improvement of SNR_{WM} [18]. Pula et al. evaluated the SNR_{WM} and reported the average value of SNR_{WM} was 4.69, while the average SNR_{WM} for this study was 7.6 for low-dose ASiR-V [19]. Besides, the findings in this study for SNR_{WM} were comparable to the study done by Paprottka et al. [16]. Cohnen et al. mentioned that the low kVp minimizes radiation dose to the eye lens and thyroid while disturbing image quality [20].

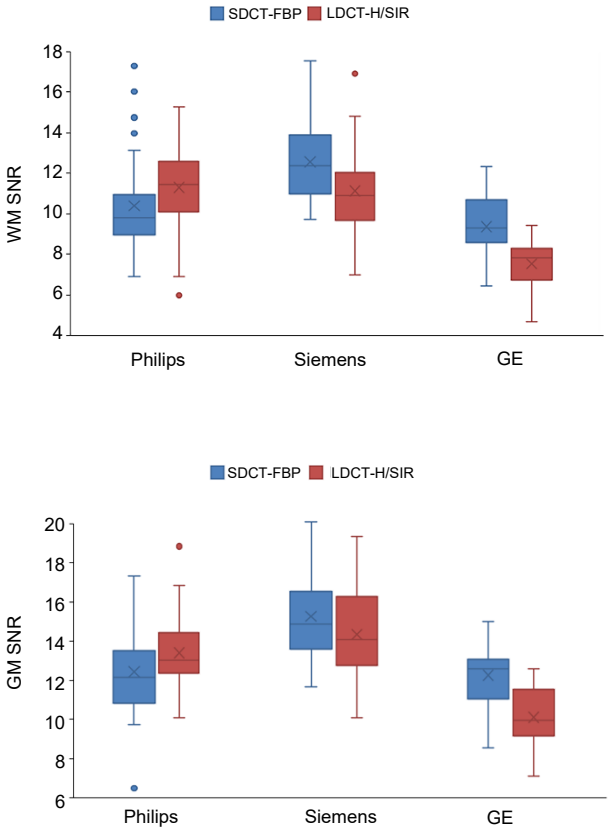

Fig. 2. SNR plots for white matter (SNR_{WM}) (top) and gray matter (SNR_{GM}) (bottom) for different CT scanners and protocols.

In the Philips scanner, the low dose combined with iDose[4] exhibited no significant improvement for GM SNR with an average SNR of 13.7 (p > 0.001), compared to the standard protocol reconstructed by FBP with an average SNR of 12.3. In Siemens scanner, the average SNR was 14.3 for the low-dose protocol combined with SAFIRE, which exhibited no significant difference compared to the standard protocol with an average of 15.4 (p > 0.001). In the GE scanner, the GM SNR for low dose combined with ASiR-V was 10.2, which was significantly lower than the standard protocol with an average SNR of 12.3 (p < 0.001).

The obtained values for GM SNR indicated no significant difference between the low-dose and standard protocols of Philips and Siemens, whereas the GE scanner showed a significant reduction in GM SNR, which may be attributed to the use of 100 kVp.

Contrast-to-Noise Ratio (CNR)

Figure 3 shows boxplots for CNR of WM-to-GM distribution for different CT scanner and CT protocols (SDCT-FBP and LDCT-H/SIR). From the findings, it is found that there was no significant difference in mean $CNR_{WM\text{-}to\text{-}GM}$ between the low-dose protocol and standard dose protocol (p > 0.001) for the three scanners. The average CNR values for the low-dose (LDCT-H/SIR) protocol were 3.12, 2.99, and 3.34 for Philips, Siemens, and GE scanners, respectively. For standard protocol (SDCT-FBP), the mean CNR values were lower: 2.8, 2.9, and 3.4 for Philips, Siemens, and GE scanners, respectively.

For $CNR_{WM\text{-}to\text{-}GM}$, there was no significant difference between low-dose and standard-dose protocols (p > 0.001). the H/SIR algorithm in LDCT demonstrated an improvement in the CNR between GM and WM compared with FBP for the Philips and Siemens scanners, indicating better contrast differentiation between WM and GM in the low-dose CT protocol. In contrast, for the GE scanner, the H/SIR algorithm showed a narrower CNR range between WM and GM, with lower CNR values compared to FBP.

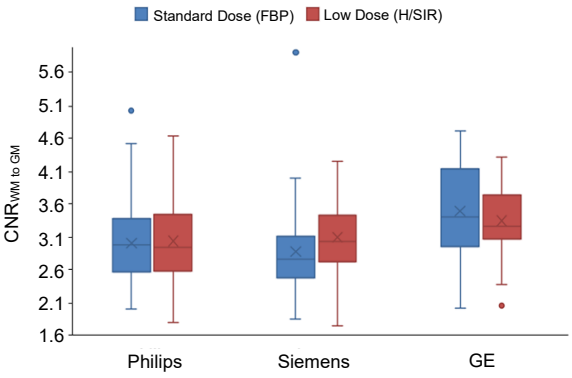

Fig. 3. $CNR_{WM\text{-}to\text{-}GM}$ for 3 scanners and different CT protocols.

Signal-to-Noise Ratio per unit Dose (SNRD)

Figure 4 shows boxplots of SNRD distribution for WM (top) and GM (bottom) between different CT scanner and CT protocols (SDCT-FBP and LDCT-H/SIR). It can be observed that there was an increase in SNRD for WM in the LDCT-H/SIR protocol across all scanners when compared to the SDCT-FBP protocol. This indicates that the LDCT-H/SIR protocol is more dose-efficient, as it provides better signal quality in white matter for the same or even reduced radiation dose. Since SNRD (and similarly, CNRD) reflects how well image quality is maintained relative to dose, a higher SNRD suggests that the protocol is capable of producing diagnostically useful images with lower radiation exposure. The statistical analysis also shows a significant difference between the low-dose protocol and standard-dose protocol (p < 0.001). The average $SNRD_{WM}$ values for low-dose protocols were 2.0, 2.0, and 1.2 for Philips, Siemens, and GE, respectively. For the standard dose protocol, the SNRD values were 1.3, 1.6, and 1.0 for Philips, Siemens, and GE, respectively.

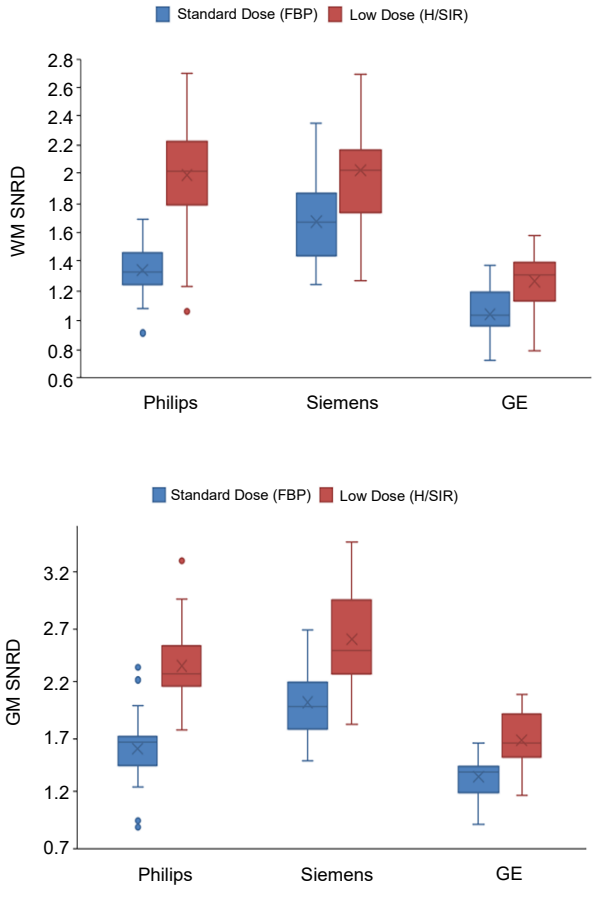

Fig. 4. SNRD plots for white matter ($SNRD_{WM}$) (top) and gray matter ($SNRD_{GM}$) (bottom) for 3 scanners and different protocols.

Contrast-to-Noise Ratio per unit Dose (CNRD)

Figure 5 shows boxplots for CNR distribution per unit dose of WM-to-GM for different CT scanners and CT protocols (SDCT-FBP and LDCT-H/SIR). The $CNRD_{WM\text{-}to\text{-}GM}$ for low-dose CT protocol was significantly enhanced compared to standard dose protocols. In the 3 scanners, the average CNRD for low-dose protocols was around 0.55, while the average CNRD for standard protocols was around 0.38.

This work demonstrated that H/SIR significantly enhanced SNRD and CNRD compared to FBP ($p < 0.001$). The improved image quality with dose reduction may be attributed to denoising that is included in ASiR-V [1] and noise subtraction, which is employed by SAFIRE and iDose^4 [6,9]. The noise reduction leads to SD value reduction, the SD in the denominator of Equations 2 and 3. Reduction in SD will increase the SNRD value, thereby maintaining the SNR and CNR after dose reduction, as shown in Eqs. (4) and (5). Since $CTDI_{vol}$ is the denominator, a reduction of the dose will increase the equation value, resulting in significantly higher SNRD and CNRD for low-dose protocols combined with standard-dose protocols using FBP ($p < 0.001$).

The finding shows SNRD and CNRD for low dose H/SIR resulted in significant enhancement of signal and contrast per radiation dose compared to the FBP image scanned using the standard dose protocol. Previous works evaluated CT image quality quantitively in comparison with radiation dose [17,21,22]. SNRD measures signal quality per unit dose, while CNRD quantifies tissue contrast relative to its surroundings at a given dose. Both metrics help optimize imaging protocols for the best balance between radiation dose and diagnostic accuracy.

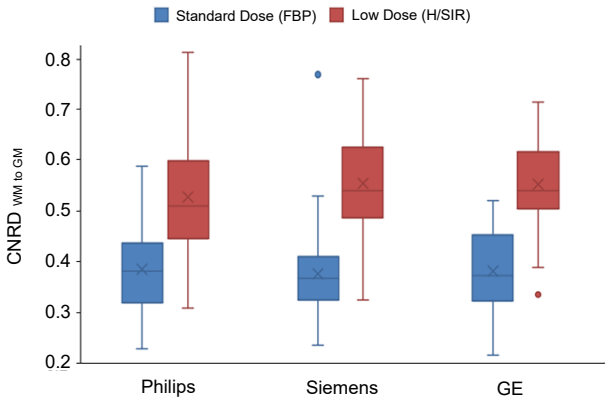

Fig. 5. $CNR_{WM\text{-}to\text{-}GM}$ for 3 scanners and different protocols.

CONCLUSION

The image quality of low-dose brain CT is preserved after the application of the H/SIR algorithm, as are the SNR and CNR of standard protocols that employ FBP, and the amount of SNRD and CNRD for the low-dose protocol compared to the standard-dose protocol. The low-dose protocol for brain CT can be employed for scanners that utilize H/SIR to reduce radiation-associated risk to patients.

ACKNOWLEDGEMENT

The authors would like to thank the Palestinian Ministry of Health and the Allmed Radiology Center for their permission for data collection.

AUTHOR CONTRIBUTION

H. Arjah, N. D. Osman, H. ALMasri, C. Anam, and M. E. Aziz equally contributed as the main contributors to this paper. All authors read and approved the final version of the paper.

REFERENCES

1. D. Qiu and E. Seeram, Radiol. - Open J. **1** (2016) 42.
2. A. Viry, C. Aberle, D. Racine *et al.*, Phys. Medica **48** (2018) 111.
3. M. Guziński, Ł. Waszczuk, and M. J. Sąsiadek, Eur. Radiol. **26** (2016) 3691.
4. H. Arjah, M. Hjouj, and F. Hjouj, in: DMIP '19 Proc. 2019 2nd Int. Conf. Digit. Med. Image Process (2019) 1.
5. J. Greffier, J. Frandon, A. Larbi *et al.*, Diagn. Interv. Imaging **100** (2019) 763.
6. Scibelli A., IDose 4 Iterative Reconstruction Technique, 2011.
7. P. De Marco and D. Origgi, J. Appl. Clin. Med. Phys. **19** (2018) 275.
8. M. Patino, J. M. Fuentes, K. Hayano *et al.*, AJR. Am. J. Roentgenol. **204** (2015) W176.
9. K. Grant and R. Raupach, Tech. Rep. (2012).
10. M. S. Chacko, D. Wu, H.S. Grewal *et al.*, J. Appl. Clin. Med. Phys. **23** (2022) 1.
11. A. Omigbodun, J. Y. Vaishnav, and S. S. Hsieh, Med. Phys. **48** (2021) 1054.
12. H. H. Harun, M. K. A. Karim, Z. Abbas *et al.*, J. Xray. Sci. Technol. **28** (2020) 893.

13. L. Wang, S. Gong, J. Yang *et al.*, J. Appl. Clin. Med. Phys. **20** (2019) 293.
14. A. Löve, R. Siemund, P. Höglund *et al.*, Acta Radiol. **55** (2014) 208.
15. C. Anam, F. Haryanto, R. Widita *et al.*, Atom Indones. **43** (2017) 55.
16. K. J. Paprottka, K. Kupfer, I. Riederer *et al.*, Sci. Rep. **11** (2021).
17. M. Lenfant, O. Chevallier, P. O. Comby *et al.*, Diagnostics **10** (2020).
18. J. Sun, H. Li, B. Wang *et al.*, BMC Med. Imaging **21** (2021) 1.
19. M. Pula, E. Kucharczyk, A. Zdanowicz *et al.*, Tomography **9** (2023) 1485.
20. M. Cohnen, H. Fischer, J. Hamacher *et al.*, Am. J. Neuroradiol. **21** (2000) 1654.
21. A. Hamza, N. D. Osman, M. Z. Ahmad *et al.*, Radiography **28** (2022) S2.
22. N. Buls, G. Van Gompel, T. Van Cauteren *et al.*, Eur. Radiol. **25** (2015) 1023.